Mathematical Models and Methods in Applied Sciences
Vol. 18, Suppl. (2008) 1249–1267

World Scientific
www.worldscientific.com

A STATISTICAL MODEL OF CRIMINAL BEHAVIOR

M. B. SHORT*, M. R. D'ORSOGNA†, V. B. PASOUR*,
G. E. TITA‡, P. J. BRANTINGHAM§,
A. L. BERTOZZI* and L. B. CHAYES*

*Department of Mathematics,
University of California — Los Angeles,
Los Angeles, CA 90095, USA

†Department of Mathematics,
California State University — Northridge,
Los Angeles, CA 91330, USA

‡Department of Criminology,
Law & Society, University of California — Irvine,
Irvine, CA 92697, USA

§Department of Anthropology,
University of California — Los Angeles,
Los Angeles, CA 90095, USA

Received 28 December 2007
Revised 1 February 2008
Communicated by N. Bellomo and F. Brezzi

Motivated by empirical observations of spatio-temporal clusters of crime across a wide variety of urban settings, we present a model to study the emergence, dynamics, and steady-state properties of crime hotspots. We focus on a two-dimensional lattice model for residential burglary, where each site is characterized by a dynamic attractiveness variable, and where each criminal is represented as a random walker. The dynamics of criminals and of the attractiveness field are coupled to each other via specific biasing and feedback mechanisms. Depending on parameter choices, we observe and describe several regimes of aggregation, including hotspots of high criminal activity. On the basis of the discrete system, we also derive a continuum model; the two are in good quantitative agreement for large system sizes. By means of a linear stability analysis we are able to determine the parameter values that will lead to the creation of stable hotspots. We discuss our model and results in the context of established criminological and sociological findings of criminal behavior.

Keywords: Crime models; reaction-diffusion equations; linear stability.

AMS Subject Classification: 35Q80, 70K99

1. Introduction

One unfortunate aspect of modern life is the presence of crime in every major urban area. However, while crime itself is ubiquitous, it does not appear to be uniformly

distributed within space and time. For example, while some neighborhoods tend to be reasonably safe, others appear far more dangerous and display dense clusters of both property and violent crimes.[7,9,21,35] Also, temporal correlations between crimes are well documented, with victims or their close neighbors often being repeatedly targeted within short periods of time.[1,25–27] These spatio-temporal aggregates of criminal occurrences are commonly referred to as crime "hotspots," and thanks to recent advances in mapping technology it is possible to track their evolution at fine spatial and temporal scales.[44] The typical lifetimes and length scales of crime hotspots are observed to vary depending upon the particular geographic, economic, or seasonal conditions present. Also, depending on the specific category of crime in question, hotspots are seen to emerge, diffuse and dissipate in ways suggestive of a structured, albeit complex, underlying dynamics. Despite this wealth of data, the efforts of law enforcement agencies towards utilizing empirical knowledge of hotspots as a tool to fight crime have been hampered by uncertainty about the predictability of such patterns.[31,34]

Many theories have been presented within the criminology community to understand why hotspots emerge in some locations rather than others, how they evolve, and how their "macroscopic" size and lifetime features are connected to the "microscopic" behaviors of offenders, victims, law enforcement agents, and the local geography. In general, crimes can only occur when a motivated offender encounters a suitable victim or target in the absence of effective security measures. In this context, the structure of the urban environment may play an important role constraining the movement of offenders and potential targets. For example, features such as traffic volume, vacant or abandoned property, population density, and the distribution of so-called crime generators impact crime patterns.[2,11,21,37,41,42]

How these numerous microscale behavioral and environmental variables combine to generate higher scale crime patterns is still a matter of debate. This is true even for the relatively simple case of residential burglary where the spatial distribution of targets (i.e. houses) remains constant over time (Fig. 1). What drives the emergence of different burglary patterns must be related not only to how offenders move within their environments, but also to how they respond to the successes and failures of their illicit activities. For example, residential burglars prefer to return to a previously burglarized house, or the ones adjacent to it, in part because it is at precisely these locations where they have good information about the types of property that might be stolen and the schedules of inhabitants.[25,46] These are known as repeat or near-repeat events, depending upon whether the burglar revisits the same home or one of its neighbors, respectively. On the other hand, the formation of crime patterns may be driven by environmental cues, where past crimes in a certain area create the image of a crime-tolerant neighborhood and lead to the proliferation of illegal activity; this is the so-called "broken windows" effect.[45]

The goal of this paper is to present a quantitative mathematical model that captures the essential dynamics of hotspot formation in light of the above sociological

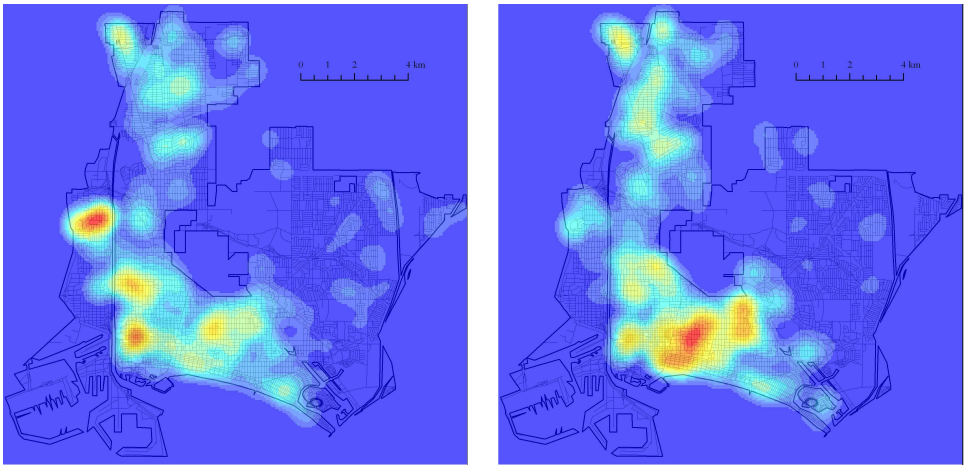

Fig. 1. Dynamic changes in residential burglary hotspots for two consecutive three-month periods beginning June 2001 in Long Beach, CA. These density maps were created using ArcGIS.

observations. We shall focus on residential burglary, which in many ways is the simplest crime type, since mobile offenders are coupled to stationary target sites, and further complexity arising from the relative movement between the agents at play may be ignored.

Our starting point is a discrete lattice system where every site corresponds to a target house. The lattice is further characterized by a series of offender agents moving from site to site according to specific rules. As we shall better illustrate in Sec. 2, burglar dynamics are strongly coupled to the level of attractiveness of target sites, with offender movement and rate of burglary biased towards more desirable locations. This bias could arise due to the fact that certain homes may indeed be easier to break into, or that these houses might simply be perceived to be better targets. The criminological and sociological effects described earlier will be incorporated into our model by letting the degree of attractiveness of each site be a dynamic, non-uniform quantity dependent upon both previous burglary events at the same location and memory effects from burglaries at neighboring sites. We will be interested in the role of this feedback loop on the dynamics and morphology of the criminal hotspots.

A continuum derivation based upon the discrete model will also be presented. Here, we coarse-grain our discrete grid so that burglars are locally described by a number density function, and interactions with the environment are embodied via coupling of this function with the coarse-grained attractiveness. Our continuum crime model will consist of two coupled reaction-diffusion-like equations describing the spatio-temporal evolution of number density and attractiveness, giving rise to hotspot formation. In the limit of large criminal populations and lattice sizes, the discrete and continuum models exhibit similar features.

2. Discrete Model

2.1. *Overview*

Our discrete burglary model consists of two components — the houses at which burglaries occur, and the criminal agents that commit these burglaries. The houses are imagined as existing on a two-dimensional lattice; for simplicity, we choose a rectangular grid with constant lattice spacing ℓ and periodic boundary conditions, though more complicated arrangements that better reflect the layout of an actual city are possible. In conjunction with the lattice spacing ℓ, a discrete time unit δt over which criminal actions will occur is also chosen. Each house is described by its lattice site $s = (i, j)$ and a quantity $A_s(t)$, which we will refer to as the attractiveness of the site. As the name implies, $A_s(t)$ is a measure of the burglars' perception of the attractiveness of the home at site s, and we model it as being equivalent to the statistical rate of burglary at site s when a burglar is present. We make no attempt to derive this attractiveness from underlying properties of the residence, such as value, security, or location. Instead, we treat the attractiveness in the spirit of collective behavior, modeling it after the sociological phenomena of repeat and near-repeat victimization and the broken windows effect discussed in the introduction. With this in mind, we let

$$A_s(t) \equiv A_s^0 + B_s(t), \tag{2.1}$$

where A_s^0 represents a static, though possibly spatially varying, component of the attractiveness, and $B_s(t)$ represents the dynamic component associated with repeat and near-repeat victimization. We shall discuss the behavior of $B_s(t)$ shortly.

The criminal agents in our model may perform one of two actions during any given simulated time interval: burglarize the house at which they are currently located, or move to one of the neighboring houses. Burglary is a random event that is characterized by a probability of occurrence for each burglar located at site s between times t and $t + \delta t$ given by

$$p_s(t) = 1 - e^{-A_s(t)\delta t}. \tag{2.2}$$

This probability is in accordance with a standard Poisson process in which the expected number of events during the time interval of length δt is $A_s(t)\delta t$. Whenever the site s is burglarized, the corresponding criminal agent is removed from the lattice at that time. This removal represents the tendency of actual burglars to flee the location of their crime after committing it. Burglars are here assumed to simply return home with their looted goods and to abstain from further crime for the time being. To simulate the removed burglars returning to active status, burglars are also generated at each lattice site at a rate Γ. This rate could in principle be spatially varying, though we will consider only the case of a uniform value.

If the criminal agent chooses not to burglarize its current location, it will then move to one of the neighboring spots on the grid. This movement will be treated as a random walk process that is biased toward areas of high attractiveness; the justification for this choice is threefold. First, it is well known that criminals predominantly

search for and victimize individuals or property in very local areas surrounding the locations that they routinely visit such as home, work, or places of recreation.[10] Second, journey-to-crime distributions generally show that the distances that criminals are willing to travel away from their primary residence to engage in crime is a monotonically decreasing function.[36] Third, in the case of residential burglary, the tendency to stay close to home often outweighs gains that might be had in traveling farther to victimize more desirable targets.[5,6] Random walk models should therefore be appropriate for studying how criminal offenders encounter criminal opportunities, because the behavior of these models is fundamentally local.

We generate the aforementioned criminal motion in our model by defining the probability of movement from site s to the neighboring site n as

$$q_{s\to n}(t) = \frac{A_n(t)}{\sum_{s'\sim s} A_{s'}(t)}, \tag{2.3}$$

where the notation $s' \sim s$ indicates all of the sites neighboring site s. Note that, by enforcing that a criminal agent will move exactly one grid-spacing ℓ within any timestep δt, we have essentially defined the movement speed of the criminals, and must choose our grid spacing ℓ and time interval δt in accordance with each other so that this speed adopts a reasonable value.

In the case of residential burglary, it has been suggested that individual residences experience an elevated risk of being re-victimized in a short period of time after a first break in.[24,25] We introduce such repeat victimization by letting the dynamic attractiveness $B_s(t)$ depend upon previous burglary events at site s. Specifically, every time a house is burglarized, we increase $B_s(t)$ for that site by a quantity θ, so that the probability for subsequent burglary events at that home increases via Eq. (2.2). It is reasonable to suppose, however, that this increased probability of burglary at a house has a finite lifetime, and as time progresses the attractiveness returns to the baseline value. We model this increase and decay according to the update rule

$$B_s(t+\delta t) = B_s(t)(1-\omega\delta t) + \theta E_s(t), \tag{2.4}$$

where ω sets a time scale over which repeat victimizations are most likely to occur and $E_s(t)$ is the number of burglary events that occurred at site s during the time interval beginning at time t.

Finally, we model near-repeat victimization[24,25] and the broken windows effect[45] by allowing $B_s(t)$ to spread spatially from each house to its neighbors. This is accomplished by modifying Eq. (2.4) to read

$$B_s(t+\delta t) = \left[(1-\eta)B_s(t) + \frac{\eta}{z}\sum_{s'\sim s} B_{s'}(t)\right](1-\omega\delta t) + \theta E_s(t), \tag{2.5}$$

where z, the coordination number, is the number of sites s' which neighbor s (four for the square lattice), and η is simply a parameter between zero and unity that

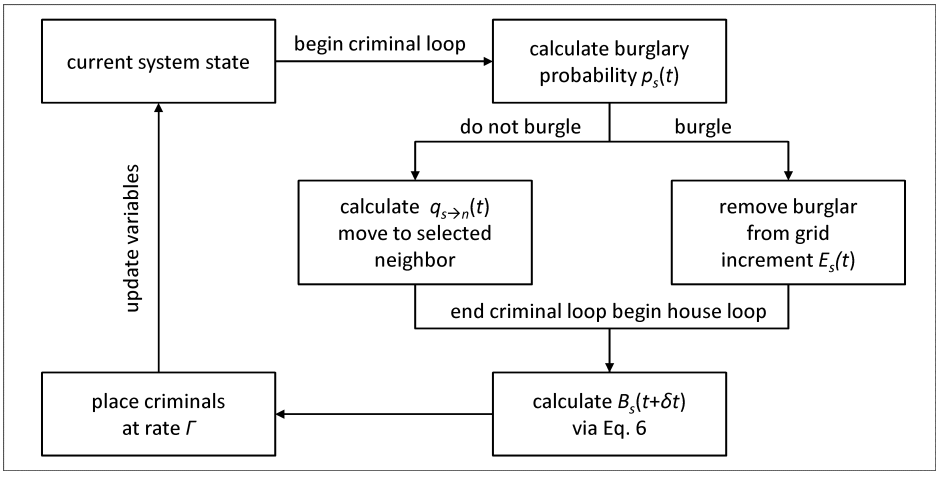

Fig. 2. Flowchart summarizing the discrete simulations.

measures the significance of neighborhood effects. Higher values of η lead to a greater degree of spreading of the attractiveness generated by any given burglary event, and lower values lead to the opposite. Equation (2.5) can be rewritten in the form

$$B_s(t+\delta t) = \left[B_s(t) + \frac{\eta\ell^2}{z}\Delta B_s(t)\right](1-\omega\delta t) + \theta E_s(t), \tag{2.6}$$

where Δ is the discrete spatial Laplacian operator

$$\Delta B_s(t) = \left(\sum_{s'\sim s} B_{s'}(t) - zB_s(t)\right) \Big/ \ell^2. \tag{2.7}$$

Figure 2 presents a visual summary of this section of the paper in the form of a flowchart.

The simplest case for our discrete system is the spatially homogeneous equilibrium solution. Here, all sites have the same attractiveness $\overline{A}$, and, on average, the same number of criminals $\overline{n}$. For the attractiveness of any given site to stay fixed, the amount by which the attractiveness decays in one timestep must be equal to the amount by which it increases due to burglary events:

$$\omega\overline{B}\delta t = \theta\ \overline{n}\ \overline{p}. \tag{2.8}$$

Similarly, in order for the number of criminals at a site to remain fixed, the number of criminals removed in one timestep (equal to the number of burglary events during that timestep) must be equal to the number of criminals produced at that site at rate Γ:

$$\overline{n}\ \overline{p} = \Gamma\delta t. \tag{2.9}$$

Table 1. Summary of parameters present in the discrete model.

Parameter name	Meaning
ℓ	Grid spacing
δt	Time step
ω	Dynamic attractiveness decay rate
η	Measures neighborhood effects (ranging from 0 to 1)
θ	Increase in attractiveness due to one burglary event
A_s^0	Intrinsic attractiveness of site s
Γ	Rate of burglar generation at each site

Putting these two equations together allows us to solve for the homogeneous equilibrium values

$$\overline{B} = \frac{\theta\Gamma}{\omega}, \qquad \overline{n} = \frac{\Gamma\delta t}{1 - e^{-\overline{A}\delta t}}. \tag{2.10}$$

The question of whether or not a system placed in this homogeneous equilibrium state will remain in it will be answered in our next section.

2.2. *Computer simulations*

Computer simulations of the model described above follow the general outline as shown in Fig. 2. The main purpose of the simulations is to give insight into the behavior of the model under various combinations of the many parameters present (see Table 1).

By varying these parameters, we observe three distinct behavioral regimes for the attractiveness field $A_s(t)$:

(1) Spatial homogeneity. In this regime, the attractiveness field has essentially the same value at all points. Any local increases in the field due to recent burglaries disappear very quickly.
(2) Dynamic hotspots. In this regime, localized spots of increased attractiveness form and remain for varying lengths of time. These spots may remain mostly fixed in space during their lifetime, or they may appear and disappear at seemingly random locations. Also, the degree of disparity in attractiveness between those areas within the hotspots and not within the hotspots depends upon the parameter choices.
(3) Stationary hotspots. In this regime, the system tends toward a steady state in which stationary spots of high attractiveness are found, surrounded by areas of extremely low attractiveness. The size of these spots varies depending upon the parameters chosen.

Some example output from the simulation for each of the cases above can be seen in Fig. 3, where we display color-maps of the attractiveness field as it evolves in time

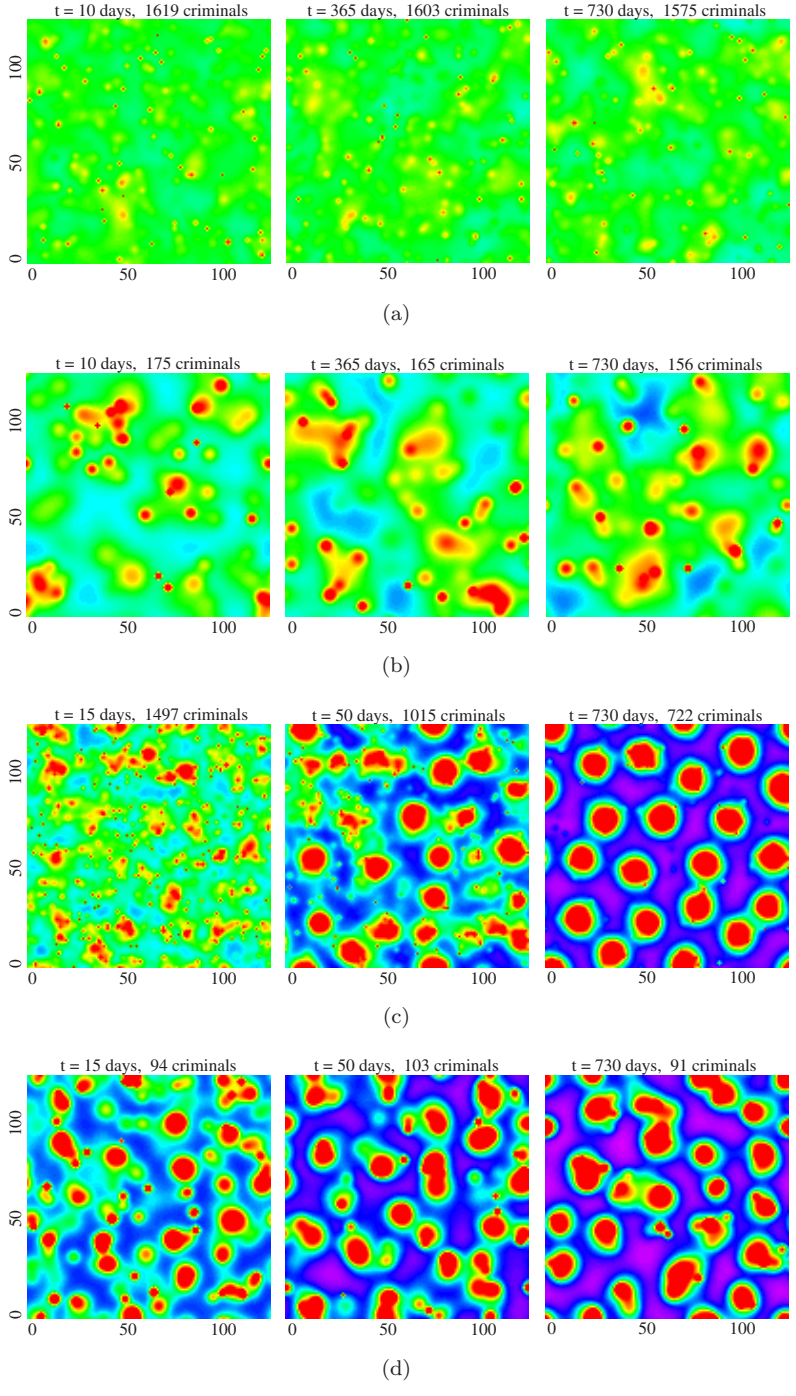

Fig. 3. Output from the discrete simulation, using parameters described in the text. For the low criminal numbers in (b) and (d), we observe dynamic hotspots. Those in (b) are more transient in nature, while those in (d) linger but display large deformations over time. For higher criminal numbers, we observe either (a) no significant hotspots, or (c) stationary hotspots.

for various sets of parameters. The spatially homogeneous equilibrium value of the dynamic attractiveness $\overline{B}$ serves as a midpoint, and is shaded in green. Other values of attractiveness follow the rainbow spectrum from violet, corresponding to $B_s = 0$, to red, corresponding to $B_s \geq 2\overline{B}$. For these particular simulations, parameters were chosen to represent possibly realistic values for those quantities which lend themselves well to estimation. All four were run with $\ell = 1, \delta t = 1/100, \omega = 1/15$, and $A^0 = 1/30$, where time may be interpreted in units of days, and distance in units of house separation. In this case, the difference between the three regimes of behavior arises by varying η, θ, and Γ: in Fig. 3(a), $\eta = 0.2, \theta = 0.56$ and $\Gamma = 0.019$; in Fig. 3(b), $\eta = 0.2$, $\theta = 5.6$, and $\Gamma = 0.002$; in Fig. 3(c), $\eta = 0.03$, $\theta = 0.56$ and $\Gamma = 0.019$; and in Fig. 3(d), $\eta = 0.03$, $\theta = 5.6$, and $\Gamma = 0.002$. All simulations were performed on a 128×128 grid, with initial conditions $B_s(0) = \overline{B}$, and the number of criminals at each site $n_s(0)$ being, on average, equal to $\overline{n}$.

We observe that the difference between those systems that exhibit behavior (2) (dynamic hotspots) and those that exhibit behavior (1) (no hotspots) and (3) (stationary hotspots) lies essentially in the relative amount of stochasticity present for the parameters chosen. Those simulations that exhibit large numbers of criminals or burglary events are more likely to fall into regimes (3) or (1) than (2), while those with low criminal numbers or low numbers of events behave in the opposite way. This seems to suggest two things: that regimes (1) and (3) are indeed two different phenomena, and that regime (2) is really only a different manifestation of either (1) or (3) arising due to finite size effects. In an effort to gain a better understanding of this, we now turn to the derivation of a continuum approximation of our discrete model.

3. Continuum Limit

3.1. *Derivation*

Let us begin the derivation of our continuum limit by analyzing the dynamics of $B_s(t)$ in greater detail. We can, as a first step, express the expected value of the dynamic attractiveness after one timestep as

$$B_s(t + \delta t) = \left(B_s(t) + \frac{\eta \ell^2}{z} \Delta B_s(t) \right) (1 - \omega \delta t) + \theta n_s(t) p_s(t). \tag{3.1}$$

We now convert $n_s(t)$ into a number density by simply dividing by ℓ^2, and renaming it $\rho(\mathbf{x}, t)$. We subtract $B_s(t)$ from both sides of the equation and then divide the equation by δt. Finally, we take the limit as both δt and ℓ become small with respect to the spatial and temporal scales of interest, with the constraints that the ratio $\ell^2/\delta t$ remain fixed with a value we define as D, and that the quantity $\theta \delta t$ also remain fixed with a value ϵ. The resulting equation gives the dynamics of the continuum version of the attractiveness,

$$\frac{\partial B}{\partial t} = \frac{\eta D}{z} \nabla^2 B - \omega B + \epsilon D \rho A. \tag{3.2}$$

The derivation of the continuum limit for $n_s(t)$ is slightly more involved. We begin with an equation expressing the expected number of agents at a site after one timestep, noting that our model demands that all of the agents that were at the site s at time t must have left the site either by moving to a neighboring site or by burglarizing the site and thereby being removed. Because of this, any agents that are present after one timestep must have either arrived there from a neighboring site after failing to burgle the neighbor, or have been generated there at rate Γ. Therefore, we conclude that

$$n_s(t+\delta t) = A_s \sum_{s' \sim s} \frac{n_{s'}(t)\left[1 - p_{s'}(t)\right]}{T_{s'}(t)} + \Gamma \delta t, \tag{3.3}$$

where, for sake of notational simplicity, we have defined

$$T_{s'}(t) \equiv \sum_{s'' \sim s'} A_{s''}(t). \tag{3.4}$$

Now, we perform an operation like that done previously when converting from Eq. (2.5) to (2.6) to write the sum in Eq. (3.3) and $T_{s'}(t)$ in terms of the discrete spatial Laplacian. We then subtract $n_s(t)$ from both sides of the equation, re-express $n_s(t)$ in terms of $\rho(\mathbf{x}, t)$, and divide by δt. Upon taking the limits of ℓ and δt as described previously, with the further constraint that $\Gamma/\ell^2 = \gamma$, we arrive at our continuum equation for criminal number density

$$\frac{\partial \rho}{\partial t} = \frac{D}{z}\vec{\nabla} \cdot \left[\vec{\nabla}\rho - \frac{2\rho}{A}\vec{\nabla}A\right] - \rho A + \gamma. \tag{3.5}$$

Equations (3.2) and (3.5) are the main results of our continuum derivation, and are of the general form of a reaction-diffusion system; such systems often lead to pattern formation.[16] The attractiveness diffuses throughout the environment while simultaneously decaying in time and reacting with the criminals to create even more attractiveness. Criminals are depleted through reactions with the attractiveness and are created at a constant rate. In addition, the criminals exhibit both diffusive motion and advective motion up gradients of attractiveness, with a speed that is inversely proportional to the local attractiveness field. This can be interpreted in a sociological sense as an example of diminishing returns; if an offender is already located at a highly attractive home, it may feel less motivation to move to neighboring houses that are, relatively speaking, not that much more attractive.

We will now point out two interesting characteristics of our continuum equations (3.2) and (3.5). First, if we integrate the steady-state version of Eq. (3.5) over our entire spatial domain, we find that the spatially averaged crime rate density is equal to γ, assuming that the criminal flux is either zero at the boundaries or is periodic. Interestingly, this means that all systems with a given γ will exhibit the same overall rate of crime at steady state, regardless of whether that crime is or is not concentrated in hotspots. Secondly, we see by integrating the steady-state version of Eq. (3.9) over our domain that our homogeneous equilibrium attractiveness value

$\overline{B}$ is in fact the spatially averaged attractiveness value for any steady-state system. In terms of our continuum parameters, this value is

$$\overline{B} = \frac{\epsilon D \gamma}{\omega}. \tag{3.6}$$

So, we can now understand in some sense why the stationary hotspots observed in our discrete simulations appear as they do, surrounded by areas of very low attractiveness: since the average attractiveness is fixed, areas of high B must be balanced by areas of low B.

As a final step, let us rewrite Eqs. (3.2) and (3.5) in a dimensionless form. We first note that a natural time scale for our model is given by $\tau \equiv 1/\omega$, as discussed previously. A characteristic length scale ℓ_c can be defined as

$$\ell_c \equiv \sqrt{\frac{D}{\omega}}, \tag{3.7}$$

which is roughly the distance over which criminal agents diffuse in the time τ it takes for the attractiveness of a newly burgled house to return to the baseline value. We therefore scale variables in the following way, denoting dimensionless versions with a tilde:

$$\tilde{A} = A/\omega, \quad \tilde{\rho} = \epsilon \ell_c^2 \rho, \quad \tilde{\mathbf{x}} = \sqrt{z}\mathbf{x}/\ell_c, \quad \tilde{t} = \omega t. \tag{3.8}$$

Using these new variables, our continuum equations can be re-expressed, now dropping the tilde notation, as

$$\frac{\partial B}{\partial t} = \eta \nabla^2 B - B + \rho A, \quad \text{and} \tag{3.9}$$

$$\frac{\partial \rho}{\partial t} = \vec{\nabla} \cdot \left[\vec{\nabla}\rho - \frac{2\rho}{A}\vec{\nabla}A \right] - \rho A + \overline{B}, \tag{3.10}$$

where $\overline{B}$ should be understood as the dimensionless version of Eq. (3.6). Note at this point that we have now transformed our original discrete system with seven parameters into a dimensionless continuum version that has only three free parameters: η, A^0, and $\overline{B}$.

Deriving continuum equations from the underlying microscale behavior of a system is a common procedure in mathematical biology.[3,4,14,15,18,19,22,33,39] It is no surprise, then, that Eqs. (3.9) and (3.10) are related to several other well-studied models. One particular model, which has a large literature in applied mathematics, is the Keller–Segel model for aggregation based on chemotaxis.[12,13,17,20,23,28,30,38,40,43] In our model, the decay of attractiveness in Eq. (3.9) includes the time derivative, which is typically suppressed in the chemotaxis models. This is because the timescale of change of attractiveness can be comparable to that of the motion of criminals, unlike in the chemotaxis problem. Moreover, in our problem we consider a decay of criminal density once crimes have occured, which is also not present in typical chemotaxis models. It would be interesting to consider some basic questions such as global existence of solutions and long-time behavior

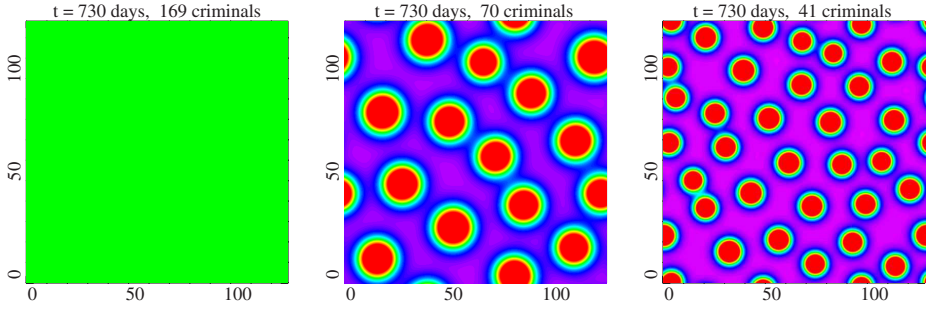

Fig. 4. Output from the continuum simulation, using parameters described in the text. Here we present only the steady-state configuration of the attractiveness. The continuum parameters used in (a) are the equivalent of the discrete parameters used in both Figs. 3(a) and 3(b), and we observe no hotspots forming. The continuum parameters used in (b) are the equivalent of the discrete parameters used in both Figs. 3(c) and 3(d), and we observe stationary hotspots with roughly the same size as those seen in Fig. 3(c). Finally, we illustrate stationary hotspots of a different size in (c).

from general initial data; these questions are outside the scope of this initial study. Another related model from population biology studies wolf and coyote territories in which scent markings are used between animals to establish buffer zones.[29,32]

3.2. *Computer simulations*

In order to verify the validity of our continuum equations, and to compare results with the discrete model, we have performed numerical simulations of Eqs. (3.2) and (3.5). Our numerical scheme is semi-implicit, using the following time-stepping algorithms in which g^m represents a quantity g at the mth timestep:

$$\left[1+\omega\Delta t-\frac{\eta D\Delta t}{z}\nabla^2\right]B^{m+1}=B^m+\epsilon D\Delta t\rho^m A^m, \tag{3.11}$$

$$\left[1+C^m-\frac{D\Delta t}{z}\nabla^2\right]\rho^{m+1}=\left[1+C^m-f^m(A)\right]\rho^m - \frac{2D\Delta t}{z}\frac{\vec{\nabla}\rho^m\cdot\vec{\nabla}A^m}{A^m}+\gamma\Delta t, \tag{3.12}$$

where

$$f(A)\equiv\frac{2D\Delta t}{z}\left[\frac{\nabla^2 A}{A}-\frac{(\vec{\nabla}A)^2}{A^2}\right]+A\Delta t, \tag{3.13}$$

C is the global maximum of $f(A)$, and Δt is the numerical timestep. Equations (3.11) and (3.12) are then solved on a computational grid with spacing h and periodic boundary conditions using standard spectral methods.[8]

Example output from the continuum simulation can be seen in Fig. 4, in which we have plotted the steady-state distribution of attractiveness with the same color

coding as used in the discrete simulations. In Figs. 4(a) and 4(b), we have used continuum parameters that are the equivalent of those used to create the plots in Fig. 3; Fig. 4(c) illustrates hotspots of a different size, using the same parameters as in Fig. 4(b) but with $\eta = 0.01$. All three are run on a 512×512 lattice with initial conditions at homogeneous equilibrium, with the exception of a few numerical gridpoints that start with a slightly higher B value. Since the parameters used to create Figs. 3(a) and 3(b) give rise to the same continuum parameters (though with a differing number of total criminals), we have only displayed the output once here (Fig. 4(a)); the same is true of the parameters from Figs. 3(c) and 3(d) (Fig. 4(b)). Note that the continuum simulation output matches the output from the discrete simulation quite well in the two cases where the number of discrete criminals is larger. This indicates that our continuum equations are indeed good approximations of the discrete system under these circumstances. As previously hypothesized, dynamic hotspots are never seen in the continuum simulations because their existence is predicated upon stochasticity and finite size effects not present in the continuum approximation. It still remains, however, to determine what distinguishes systems that, in the continuum sense at least, do not exhibit hotspots from those that do. In the following section we perform a linear stability analysis of the system in order to address this question.

3.3. *Linear stability analysis*

For simplicity, let us consider Eqs. (3.9) and (3.10) with a spatially uniform value for A^0. The homogeneous equilibrium solutions are found to be

$$\overline{A} = A^0 + \overline{B} \quad \text{and} \quad \overline{\rho} = \frac{\overline{B}}{A^0 + \overline{B}}. \tag{3.14}$$

We now examine the behavior of solutions of the form

$$A(\mathbf{x}, t) = \overline{A} + \delta_A e^{\sigma t} e^{i\mathbf{k}\cdot\mathbf{x}}, \tag{3.15}$$

$$\rho(\mathbf{x}, t) = \overline{\rho} + \delta_\rho e^{\sigma t} e^{i\mathbf{k}\cdot\mathbf{x}}. \tag{3.16}$$

We only consider here perturbations of A and ρ with the same wavenumber $\mathbf{k}$, as it can be easily shown that all perturbations of differing wavenumber will decay in time. Upon substitution into our differential equations, we obtain the following linearized system:

$$\begin{bmatrix} -\eta|\mathbf{k}|^2 - 1 + \overline{\rho} & \overline{A} \\ \dfrac{2\overline{\rho}}{\overline{A}}|\mathbf{k}|^2 - \overline{\rho} & -|\mathbf{k}|^2 - \overline{A} \end{bmatrix} \begin{bmatrix} \delta_A \\ \delta_\rho \end{bmatrix} = \sigma \begin{bmatrix} \delta_A \\ \delta_\rho \end{bmatrix}, \tag{3.17}$$

which we can solve to find σ. Linear instability of the system is present for all values of σ that are greater than zero (Fig. 5), which, for our system, will occur at

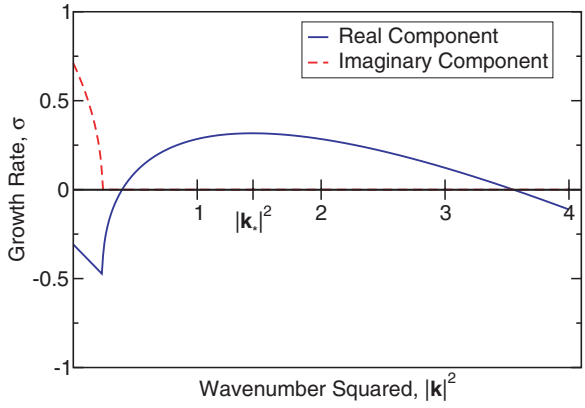

Fig. 5. An example of the growth rate σ for a linearly unstable system, as found by solving Eq. (3.17). The imaginary component is only nonzero over wavenumbers for which the real component is negative, indicating no growing oscillations in the system. The real component is positive over a finite band of wavenumbers, and has a peak at a value $|\mathbf{k}_*|^2$; this maximally growing mode should set the final size of hotspots.

wavenumbers $\mathbf{k}$ for which the determinant of the coefficient matrix in Eq. (3.17) is negative:

$$\eta|\mathbf{k}|^4 - (3\overline{\rho} - \eta\overline{A} - 1)|\mathbf{k}|^2 + \overline{A} < 0. \tag{3.18}$$

This inequality will at most hold true for a finite band of wavenumbers, and only if the parameters of the problem are such that

$$3\overline{\rho} - \eta\overline{A} - 1 > 2\sqrt{\eta\overline{A}}\ . \tag{3.19}$$

The inequality in Eq. (3.19) can be used, then, to differentiate between systems that will and will not exhibit instabilities, based upon the three quantities A^0, η, and $\overline{B}$. We can further dissect Eq. (3.19) by noting that, for any instability to be possible, it must be the case that

$$\overline{B} > \frac{A^0}{2}. \tag{3.20}$$

If this inequality is held, then any η that satisfies

$$\eta < \frac{3\overline{\rho} + 1 - \sqrt{12\overline{\rho}}}{\overline{A}} \tag{3.21}$$

will lead to an instability.

A deeper understanding of the inequality of Eq. (3.19) can be found by examining the case in which $A^0 = 0$. Under this regime, the inequality simplifies to

$$\frac{\epsilon\eta D}{\omega}\frac{\gamma}{\omega} < 4 - 2\sqrt{3}. \tag{3.22}$$

The fractional quantity $\epsilon\eta D/\omega$ can be interpreted as the area of influence of any given burglary event, i.e. the area over which the increase in B from a burglary

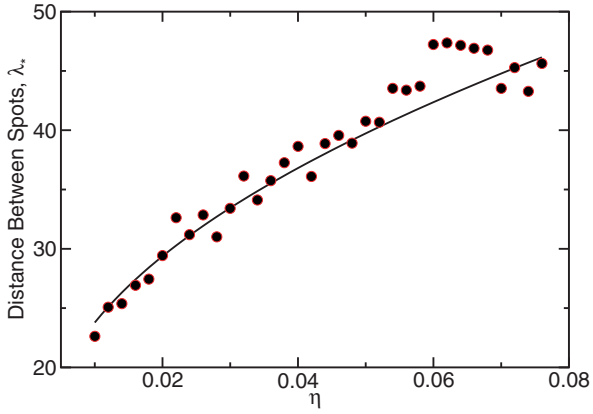

Fig. 6. A comparison between hotspot separation as measured in the continuum simulations (red dots) and as predicted by our linear stability analysis via $\lambda_* = 2\pi/|\mathbf{k}_*|$, with $|\mathbf{k}_*|$ given by Eq. (3.23) (black line). We observe good agreement between the two as we vary the parameter η, though edge effects arising from our choice of periodic boundary conditions may be affecting the results at large values of λ_*.

event can be measurably felt before it decays away. The other quantity, γ/ω, can be interpreted as the average number of events per area in the time τ at steady-state; its inverse is therefore the average area per event at steady-state. The inequality, then, indicates that isolated burglary hotspots will only occur at steady-state if the average area per event is greater than the area of influence of any single event. In other words, isolated spots of high B can only exist if these spots are far enough away from each other that they do not interact.

If the system is indeed unstable, there will be a wavenumber $\mathbf{k}_*$ that exhibits the fastest growth rate of all the unstable modes. This maximally growing mode can be shown to be given by

$$|\mathbf{k}_*|^2 = (1-\overline{A})/(1-\eta) - \overline{\rho}(5-\eta)/(1-\eta)^2 + \sqrt{\eta(1+\eta)^2\overline{\rho}\left[\left(\overline{A}(3-\eta)-2\right)(1-\eta)+2\overline{\rho}(3-\eta)\right]}/\eta(1-\eta)^2, \qquad (3.23)$$

and should set the scale $\lambda_* = 2\pi/|\mathbf{k}_*|$ for hotspot separation at steady-state. To test this prediction, we ran the continuum simulation with the same parameters used to create Fig. 4(b), while varying the value of the parameter η. Figure 6 compares the hotspot separation as determined by the output of these simulations with the separation that is predicted analytically by Eq. (3.23); the agreement is quite good.

We now have a very good understanding of the output of the continuum (and to some extent, the discrete) simulations. For the parameters used to create Fig. 4(a), Eq. (3.19) does not hold, indicating that the homogeneous equilibrium solution is stable, which is what we observe. For Figs. 4(b) and 4(c) the opposite is true, and we indeed see hotspots emerging at scales that we can predict using Eq. (3.23).

4. Conclusions

We re-emphasize at this point that the model described herein has been constructed based upon the empirically known behavior of criminal offenders. First, based on the fact that burglars most often victimize areas near where they live, work, or spend free time, we have chosen to model their movement as a biased random walk, as the behavior of such a model is fundamentally local in space. Second, as it is clear that repeat victimization plays an important role in crime pattern generation, we have developed the idea of an attractiveness field that not only determines the rate of burglary at a given site, but is also influenced by past burglary events and serves as the source of bias in the criminals' movement. Finally, we have introduced spatio-temporal scales for hotspots by allowing our attractiveness field to diffuse within a neighborhood while simultaneously decaying in time. We thus are able to construct a model where the two main variables at play, offender position (or density in the continuum model), and biasing attractiveness field, create nonlinear feedback loops which originate patterns of aggregation, reminiscent of actual crime hotspots.

This sociologically based model accomplishes our chief goal of exhibiting qualitative similarity with the hotspots observed in actual cities. However, there has been no comparison as of yet between the quantitative aspects of the hotspots generated thereby and empirical crime data. This is partly because of the difficulty in developing a rigorous metric by which such a comparison could be made. To wit, there are numerous quantities that can be measured in both our simulation output and empirical burglary data that could serve as such a rubric: the probability distribution for number of burglaries per house over a prescribed period of time, the distribution of time to next event for houses within a fixed distance of a burglary event, any number of tests for spatiotemporal clustering of burglary events, etc. Choosing which one of these measures to focus our attention toward is a work in progress.

In addition to this difficulty in determining the appropriate metric for comparison is the fact that there are other variables acting within the empirical data that are not accounted for in the model, e.g. police presence and other security measures. It is a fact that police departments often distribute crime control resources based upon recent criminal activity, which may shorten the lifetime of hotspots, cause them to relocate, or destroy them altogether. Despite these many difficulties, however, we feel confident that the parameters of our model could be chosen to give good agreement between simulation and real data.

Another area of further inquiry involves incorporating inhomogeneities into the computer simulations. For example, it would be very interesting to construct the background attractiveness field A^0 or the burglar generation rate Γ by taking into account the characteristics of a specific city location (neighborhood income levels, security measures installed, proximity to crime generating or deterring centers, physical hindrances to the spread of A, police response times and methods). In a

similar vein, constructing realistic urban lattices upon which to run our simulations will be very important in the future, and allow for much better comparisons between the simulation and data, as well as possibly providing enhanced predictive capability.

In the end, we feel that the ideas presented here will form the basis for a better understanding of why and how crime hotspots form and of their underlying dynamics. This knowledge may eventually prove useful for developing better methods of crime prediction and prevention and allow the police and other security agencies to more effectively control resource allocation from day to day.

Acknowledgments

The authors wish to thank the Los Angeles and Long Beach police departments, Joe Kuhns of the LAPD, Roy Stone of the LBPD, and Tom Chou of UCLA for helpful discussions, NSF grants BCS-0527388 and DMS-0719462, and ARO grant MURI-50363-MA-MUR.

References

1. L. Anselin, J. Cohen, D. Cook, W. Gorr and G. Tita, *Criminal Justice* 2000, Vol. 4 (National Institute of Justice, 2000), pp. 213–262.
2. D. Beavon, P. L. Brantingham and P. J. Brantingham, *Crime Prevention Studies*, Vol. 2 (Willow Tree Press, 1994), pp. 115–148.
3. N. Bellomo, A. Bellouquid, J. Nieto and J. J. Soler, Multicellular growing systems: Hyperbolic limits towards macroscopic description, *Math. Mod. Meth. Appl. Sci.* **17** (2007) 1675–1693.
4. M. Bendahmame, K. H. Karlsen and J. M. Urbano, On a two-sidely degenerate chemotaxis model with volume-filling effects, *Math. Mod. Meth. Appl. Sci.* **17** (2007) 783–804.
5. W. Bernasco and F. Luykx, Effects of attractiveness, opportunity and accessibility to burglars on residential burglary rates of urban neighborhoods, *Criminology* **41** (2003) 981–1001.
6. W. Bernasco and P. Nieuwbeerta, How do residential burglars select target areas? A new approach to the analysis of criminal location choice, *Brit. J. Criminology* **45** (2005) 296–315.
7. A. E. Bottoms and P. Wiles, *Crime, Policing and Place: Essays in Environmental Criminology* (Routledge, 1992), pp. 11–35.
8. J. P. Boyd, *Chebyshev and Fourier Spectral Methods*, 2nd edn. (Dover, 2001).
9. P. J. Brantingham and P. L. Brantingham, *Patterns in Crime* (Macmillan, 1984).
10. P. J. Brantingham and P. L. Brantingham, *Environmental Criminology*, 2nd edn. (Waveland Press, 1991), pp. 27–54.
11. P. J. Brantingham and P. L. Brantingham, Criminality of place: Crime generators and crime attractors, *Euro. J. Criminal Policy Res.* **3** (1995) 5–26.
12. M. Burger, M. Di Francesco and Y. Dolak-Struss, The Keller–Segel model for chemotaxis with prevention of overcrowding: Linear vs. nonlinear diffusion, *SIAM J. Math. Anal.* **38** (2006) 1288–1315.
13. H. M. Byrne and M. R. Owen, A new interpretation of the Keller–Segel model based on multiphase modelling, *J. Math. Biol.* **49** (2004) 604–626.

14. F. A. Chalub, Y. Dolak-Struss, P. Markowich, D. Oeltz, C. Schmeiser and A. Soref, Model hierarchies for cell aggregation by chemotaxis, *Math. Mod. Meth. Appl. Sci.* **16** (2006) 1173.
15. F. A. Chalub, P. A. Markovich, B. Perthame and C. Schmeiser, Kinetic models for chemotaxis and their drift-diffusion limits, *Mon. Math.* **142** (2004) 123.
16. M. C. Cross and P. C. Hohenberg, Pattern formation outside of equilibrium, *Rev. Mod. Phys.* **65** (1993) 851–1112.
17. M. del Pino and J. Wei, Collapsing steady states of the Keller–Segel system, *Nonlinearity* **19** (2006) 661–684.
18. Y. Dolak and C. Schmeiser, Kinetic models for chemotaxis: Hydrodynamic limits and spatio temporal mechanisms, *J. Math. Biol.* **51** (2005) 595–615.
19. R. Erban and H. G. Othmer, From individual to collective behaviour in chemotaxis, *SIAM J. Appl. Math.* **65** (2004) 361–391.
20. C. Escudero, The fractional Keller–Segel model, *Nonlinearity* **19** (2006) 2909–2918.
21. M. K. Felson, *Crime and Nature* (Sage Publications, 2006).
22. F. Filbet, P. Laurençot and B. Perthame, Derivation of hyperbolic models for chemosensitive movement, *J. Math. Biol.* **50** (2005) 189–207.
23. M. A. Herrero and J. J. L. Velázquez, Chemotactic collapse for the Keller–Segel model, *J. Math. Biol.* **35** (1996) 177–194.
24. S. D. Johnson, W. Bernasco, K. J. Bowers, H. Elffers, J. Ratcliffe, G. Rengert and M. Townsley, Space-time patterns of risk: A cross national assessment of residential burglary victimization, *J. Quantitative Criminology* **23** (2007) 201–219.
25. S. D. Johnson, K. Bowers and A. Hirschfield, New insights into the spatial and temporal distribution of repeat victimisation, *Br. J. Criminology* **37** (1997) 224–244.
26. S. D. Johnson and K. J. Bowers, The burglary as clue to the future: The beginnings of prospective hot-spotting, *Eur. J. Criminology* **1** (2004) 237–255.
27. S. D. Johnson and K. J. Bowers, Domestic burglary repeats and space-time clusters: The dimensions of risk, *Eur. J. Criminology* **2** (2005) 67–92.
28. E. F. Keller and L. A. Segel, Initiation of slime mold aggregation viewed as an instability, *J. Theor. Biol.* **26** (1970) 399–415.
29. M. A. Lewis, K. A. J. White and J. D. Murray, Analysis of a model for wolf territories, *J. Math. Biol.* **35** (1997) 749–774.
30. S. Luckhaus and Y. Sugiyama, Large time behavior of solutions in super-critical cases to degenerate Keller–Segel systems, *Math. Model. Numer. Anal.* **40** (2006) 597–621.
31. L. McLaughlin, S. D. Johnson, D. Birks, K. J. Bowers and K. Pease, Police perceptions of the long and short term spatial distribution of residential burglary, *Int. J. Police Sci. Management* **9** (2007) 99–111.
32. P. R. Moorcroft, M. A. Lewis and R. Crabtree, Mechanistic home range models predict patterns of coyote territories in yellowstone, *Proc. Roy. Soc. London B* **273** (2006) 1651–1659.
33. H. G. Othmer and T. Hillen, The diffusion limit of transport equations II: Chemotaxis equations, *SIAM J. Appl. Math.* **62** (2002) 1222–1250.
34. J. H. Ratcliffe, Crime mapping and the training needs of law enforcement, *Eur. J. Criminal Policy Res.* **10** (2004) 65–83.
35. G. F. Rengert, *Crime, Policing and Place: Essays in Environmental Criminology* (Routledge, 1992), pp. 109–117.
36. G. F. Rengert, A. R. Piquero and P. R. Jones, Distance decay reexamined, *Criminology* **37** (1999) 427–445.
37. D. Roncek and R. Bell, Bars, blocks and crime, *J. Environ. Sys.* **11** (1981) 35–47.

38. T. Senba, Type II blowup of solutions to a simplified Keller–Segel system in two-dimensional domains, *Nonlinear Anal. Th. Meth. Appl. Int. Multidisciplinary J. Ser. A: Th. Meth.* **66** (2007) 1817–1839.
39. A. Stevens, The derivation of chemotaxis equations as limit dynamics of moderately interacting stochastic many-particles systems, *SIAM J. Appl. Math.* **61** (2002) 183–212.
40. Y. Sugiyama, Global existence in sub-critical cases and finite time blow-up in super-critical cases to degenerate Keller–Segel systems, *Differential and Integral Equations. Int. J. Th. Appl.* **19** (2006) 841–876.
41. G. Tita, J. Cohen and J. Engberg, An ecological study of the location of gang "set space," *Social Problems* **52** (2005) 272–299.
42. G. Tita and G. Ridgeway, The impact of gang formation on local patterns of crime, *J. Res. Crime Delinquency* **44** (2007) 208–237.
43. J. J. L. Velázquez, Well-posedness of a model of point dynamics for a limit of the Keller–Segel system, *J. Diff. Eqs.* **206** (2004) 315–352.
44. W. F. Walsh, Compstat: An analysis of an emerging police managerial paradigm, *Policing* **24** (2001) 347–362.
45. J. Q. Wilson and G. L. Kelling, Broken windows and police and neighborhood safety, *Atlantic Mon.* **249** (1982) 29–38.
46. R. Wright and S. Decker, *Burglars on the Job* (Northeastern Univ. Press, 1994).